engineering proceedings

Proceeding Paper

DECI: A Differential Entropy-based Compactness Index for Point Clouds Analysis. Method and Potential Applications †

Emmanuele Barberi [1],*, Filippo Cucinotta [1], Per-Erik Forssén [2] and Felice Sfravara [1]

[1] Department of Engineering, University of Messina, Italy
[2] Department of Electrical Engineering, University of Linköping, Sweden
* Correspondence: emmanuele.barberi@unime.it;
† Presented at the 4th International Electronic Conference on Applied Sciences title, online, 27 October-10 November 2023.

Abstract: This article introduces the Differential Entropy-based Compactness Index (*DECI*), a new metric for synthetically describing the spatial distribution of point clouds. *DECI* is founded on the differential entropy (DE) of point clouds and if they depict a moving object distribution, the index enables real-time monitoring. Historical data analysis allows studying *DECI* trends and average values in defined intervals. Multiple practical applications are suggested, including risk assessment, congestion measurement, traffic control (including autonomous systems), infrastructure planning, crowd density, and health analysis. *DECI*'s real-time and historical insights are valuable for decision-making, system optimization, and hold potential as a feature in Machine Learning applications.

Keywords: point clouds; 3D geometry distribution assessment; compactness index; differential entropy; risk assessment; real-time;

Citation: Barberi, E.; Cucinotta, F.; Forssén, P.-E.; Sfravara, F. DECI: A Differential Entropy-based Compactness Index for Point Clouds Analysis. Method and Potential Applications. **2023**, *5*, x. https://doi.org/10.3390/xxxxx

Academic Editor(s):

Received: date
Accepted: date
Published: date

1. Introduction

1.1. Point Clouds

Point clouds serve as a potent representation tool for three-dimensional (3D) geometry, finding applications across a diverse spectrum of industries. This technique hinges upon a collection of points in the 3D space, capturing intricate details of object surfaces and their spatial arrangement. The acquisition of requisite data to construct point clouds can be achieved through a range of methodologies, encompassing advanced 3D scanners [1,2], laser scanners [3,4], as well as techniques like tomography [5] and photogrammetry [6]. Point clouds are commonly generated using 3D scanners to capture intricate details of physical objects and environments, making them valuable in in fields like industrial design, architecture, medicine, and digital art. They can also be created from 3D CAD models, allowing for assessment of virtual designs. Point clouds extend beyond representing objects and find utility in broader contexts, such as transportation systems, where the possibility to consider the vehicles as points, could help to optimize traffic flow and routes.

1.2. Litterary review

Several methodologies have been devised to articulate point clouds and thereby extract substantial insights. These methodologies encompass density-based [7] and shape-based [8,9] approaches, each tailored towards encapsulating specific facets of point spatial distribution. Within the gamut of density-based approaches, the employment of density histograms [10] emerges to measure the concentration of points within distinct spatial realms. This method furnishes a valuable tool in detecting point clusters or regions of elevated density within the point cloud. Furthermore, delving into the shape of the point cloud entails the extraction of geometric attributes, encompassing ellipticity, angular aperture, and analogous measures associated with point morphology. This genre of approach finds applicability in elucidating point clouds that delineate objects of distinct configurations. Point clouds analysis with entropy, specifically with differential entropy (DE) [11–13], offers a unique perspective on characterizing their spatial distribution and complexity. Entropy in point clouds measures the uncertainty or randomness in the arrangement of points in 3D space, aiding in assessing information, regularity, or disorder in the data. DE analyzes each point's entropy individually, offering a detailed view of their contribution to spatial complexity. Studying point clouds through DE allows for a nuanced understanding, enhancing context-aware analyses across diverse applications and research domains.

1.3. Aim of the work

This work aims to introduce the "Differential Entropy-based Compactness Index" (*DECI*), as an innovative metric, and its potential applications. The index not only delineates the spatial distribution of points but also furnishes a novel lens through which to appraise risk, congestion, and the structural aspects within point clouds. Applications span from controlling maritime, aerial, and road traffic (inclusive of autonomous driving) to scrutinizing crowd density in public and indoor spaces, thus finding an amenable environment within the proposed framework. *DECI* also exhibits versatility across domains like health, biology, and sports analysis, generating a broad spectrum of possible utility.

2. Materials and Methods

2.1. Differential Entropy

In the context of point clouds, denoted as P, comprising a collection of points (p_n), the total DE (H) for a multivariate normal distribution is defined as the summation of individual differential entropies (h_i) associated with each point (p_n). It is also useful to use the average value ($\overline{H}$) of the total DE, by dividing H by the total number of points (n). This computation is expressed by the formula [14]:

$$h_i(p_k) = \frac{1}{2} ln[(2\pi e)^N |\Sigma(p_k)|] \quad (1)$$

Here, N represents the dimensionality of the data, and $\Sigma(p_k)$ denotes the sample covariance matrix related to the k points p_k within the neighborhood (ϙ). To simplify the methodology, N=2 is considered (points on a plane). Consequently, $\overline{H}$ is given by:

$$\overline{H}(P) = \frac{\sum_1^n h_i(p_k)}{n} \quad (2)$$

The aforementioned sample, from which the covariance matrix is derived, comprises the points contained within ϙ of each p_n. ϙ is considered circular, centered at each point with a radius r. Depending on the k value within each ϙ, three distinct scenarios arise:

1. If $k \geq 3$, the generalized variance is positive.
2. If $k = 2$, the determinant is null, rendering the use of multivariate differential entropy as a measure of disorder unfeasible. In this case, the system can be described as univariate, with the index of dispersion represented by the variance along an axis passing between the two points.
3. If $k = 1$, the variance is null, and the entropy itself is null, as there is only one element in the neighborhood.

Given these considerations, in the case of a planar distribution, the differential entropy can be expressed as:

1. $$k = 1 \rightarrow h_i = 0 \quad (3)$$

2. $$k = 2 \rightarrow h_i = \frac{1}{2} ln\left[(2\pi e)^2 \left(\sigma_x + \sigma_y\right)^2 + 1\right] \quad (4)$$

3. $$k \geq 3 \rightarrow h_i = \frac{1}{2} ln[(2\pi e)^2 \, |\Sigma(p_k)| + 1] \quad (5)$$

As it can be seen in the previous formulas, authors suggest these modifications to the DE formulas. In eq. 4, the determinant of the covariance matrix is replaced by the square of the sum of the x variance (σ_x) and y variance (σ_y) of the k points, the DE, as defined, remains invariant to both rotation and translation. To ensure h_i remains positive, the authors added a constant value of 1 to the argument of the logarithm. The addition of the term 1 to the formula will be better discussed at the end of the next paragraph.

2.2. DECI

In seeking an index that attains a value of zero when the point set distribution is adequately sparse and progressively increases as the points draw closer to each other, the authors have defined *DECI* as follows:

$$DECI(P) = \frac{\sum_1^n deci_i(p_k)}{n} \quad (6)$$

Where:

$$deci_i(p_k) = \begin{cases} 0 & if \quad h_i(p_k) = 0 \\ \dfrac{1}{h_i(p_k)} & if \quad h_i(p_k) \neq 0 \end{cases} \quad (7)$$

Thus, in accordance with the concepts of h_i and $\bar{H}$ for a point set distribution, a global compactness value (*DECI*) is derived in a manner that is proportionate to the sum of individual values (*deci*) associated with each point. The authors' decision to introduce the constant value of 1 into the formula guarantees that the argument of the logarithm is consistently greater than one, ensuring that h_i remains positive or, at least, zero.

This adjustment is particularly crucial in light of the potential applications of the proposed index (*DECI*). Indeed, when contemplating applications, especially within the realm of congestion and risk associated with transportation systems, it becomes imperative to maintain the *DECI* with a positive value. This design ensures that *DECI* remains at zero in the absence of risk and consistently increases as the level of risk escalates.

2.3. Experiments

To show *DECI*'s characteristics and potential, tests were performed on random 2D point clouds. We examined how *DECI* behaves with changing distributions and varying *r*. The experiments focused on a random distribution called D1, comprising 100 points within a box defined by lower limits of 0 and upper limits of 500 on both the X and Y axes. *DECI* was calculated using different *r* for each point (*r* values: 10, 20, 30, 40, 50, 60, 70).

In another scenario, each point was assigned an *r* between 0 and 50, with no specific measurement units. It's important to note that these units correspond to physical lengths.

While a broader search radius, theoretically infinite, can describe the entire point distribution, it's more relevant in transportation systems to identify points (representing vehicles, ships, aircraft, drones, etc.) clustering in specific areas. Such aggregations may indicate potential congestion and/or hazards.

3. Results

D1 was examined with a uniform *r* assigned to each point. Figure 1 (a) illustrates the *deci* values for each point and the resulting *DECI* value for the distribution when using a *r* equal to 10. Figure 1 (b) focuses on a specific region within the same case, providing insight into how *deci* functions. It is evident that isolated points (those without any other points in their vicinity) have *deci* values of 0. Additionally, in the case of the two pairs of points nearest to each other, *deci* is higher for the upper pair compared to the lower one.

It should be noted that the color of the circles is not related to the *deci*, but is chosen randomly to better distinguish the various ϱ.

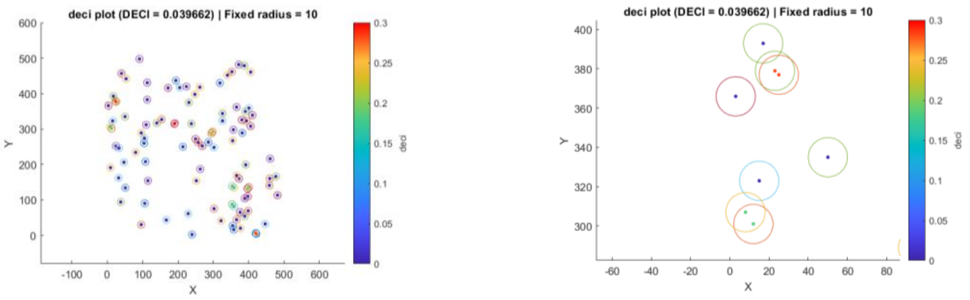

(**a**) (**b**)

Figure 1. (**a**) *deci* plot of D1 with a fixed radius whose value is 10; (**b**) A detail of a specific area.

Figure 2 displays two examples of D1 with different search radius values. It is possible to see *DECI* increasing.

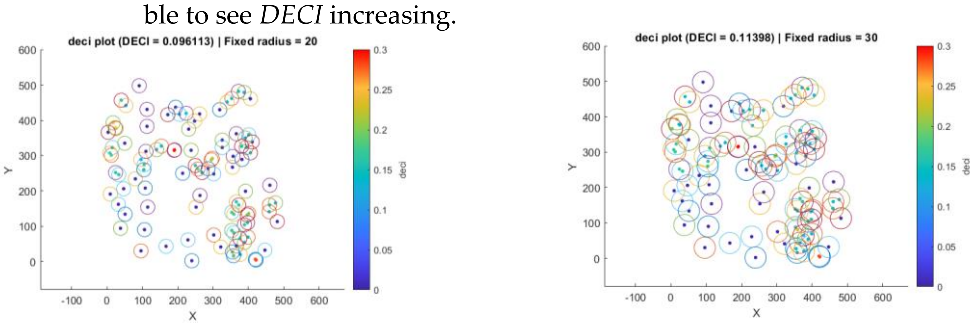

(**a**) (**b**)

Figure 2. (a) deci values of D1 with search radius 20; **(b)** deci values of D1 with search radius 30.

Figure 3 depicts a specific area of the above figures as example. The figure illustrates how the *deci* values vary for each point as the radius changes.

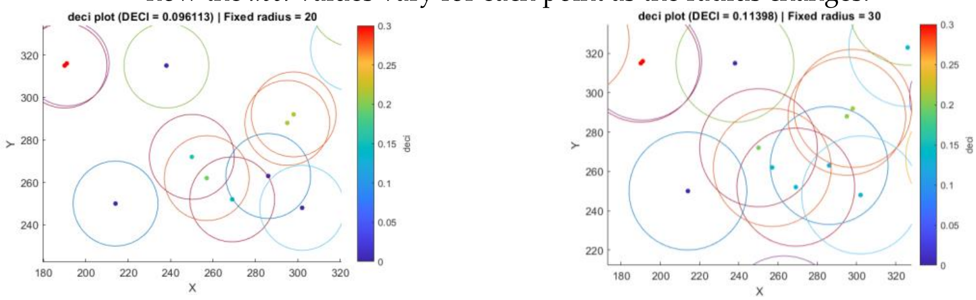

(**a**) (**b**)

Figure 3. (a) Detail of D1 with search radius 20; **(b)** Detail of D1 with search radius 30.

An analysis of the point clouds was also conducted using the original differential entropy formulas in order to compare the proposed method with the existing one. Table 1 displays the values of *DECI* and $\overline{H}$ for D1 as the radius changes and their trend is shown in Figure 4 (a). It also includes the *DECI* value related to the entire distribution (with an infinite *r*, as mentioned earlier) for comparison.

Table 1. Values of *DECI* and $\overline{H}$ calculated for D1 as the *r* changing.

Radius	**10**	**20**	**30**	**40**	**50**	**60**	**70**	**+Inf**
DECI	0.0397	0.0961	0.1140	0.1162	0.1139	0.1086	0.1087	0.0788
$\overline{H}$	39.2756	248.7611	204.9992	207.1805	244.8835	134.2913	152.7676	12.6881

An example of D1 with variable radius is shown in Figure 4 (b).

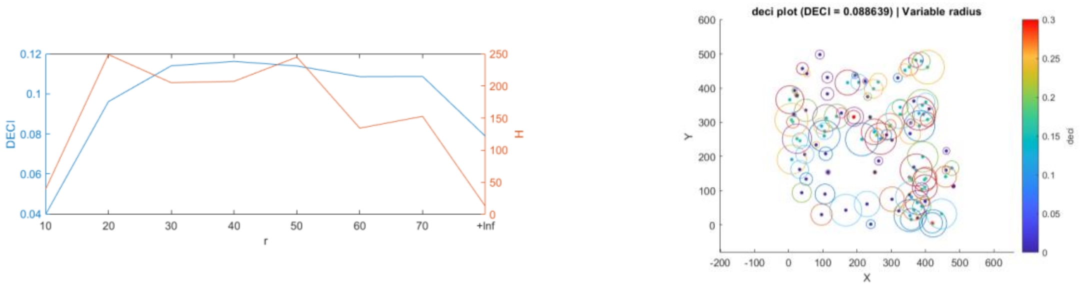

(**a**) (**b**)

Figure 4. (a) Comparison between *DECI* and $\overline{H}$; **(b)** *deci* plot of D1 with variable *r* and related *DECI*'s value.

4. Discussion

Observing Table 1, it can be noted that, as the *r* increases, *DECI* exhibits an initially rising and subsequently falling trend. Specifically, with a *r* equal to 0, *deci* values are, by definition, all set to zero, resulting in a null *DECI*. Conversely, with a theoretically infinite search radius, *DECI* tends to describe the entire point cloud, yielding identical *deci* values for all points. Looking at the $\overline{H}$ results, the trend is unstable. In fact, sudden increases and decreases are noted with an absolute minimum when the *r* is infinite. On the contrary, the *DECI* trend appears to be more stable and coherent. As the search radius expands, the influence of point-to-point interactions on *deci* values becomes apparent, as depicted in Figure 2 and Figure 3. Using different search radii for individual points, as shown in Figure 4 (b) , is highly important in specific practical applications of this method. Whether a point represents a mode of transportation or a generic entity, it has inherent properties reflecting real-world attributes. Tailoring the search radius for each point can mirror a physical characteristic, like speed or size, affecting its interactions with other points. For example, in the context of ships at sea, the search radius might depend on factors like ship size and speed. Larger and faster ships could pose a greater risk of interaction due to their unique attributes. Similarly, analyzing a football team's evolution during a match and its impact on the game's outcome can be explored by studying changes in DECI.

5. Conclusions

In this study, the *DECI* index for point cloud description has been introduced. It has been demonstrated that it could primarily serve as a risk or congestion index in the field of transportation. The influence of a different radius for each point is considered essential, as the points may represent a system's schematic, and each system possesses certain physical properties that can be reflected through the search radius. Beyond the transportation and logistics domain, entropy-based analyses and the *DECI* index could find applications in the medical field (for tracking the position and movement of specific cell groups), materials science (for analyzing the distribution and size of defects), and human (crowd dynamics and sports) and animals behavior analysis. Real-time analysis is also possible, as well as the evaluation of *DECI* trends over time.

Author Contributions: "Conceptualization, E.B. and F.C.; methodology, E.B., F.C., P.F. and F.S.; software, E.B.; validation, E.B., F.C. and F.S.; formal analysis, F.S.; investigation, E.B. and F.C.; resources, P.F.; data curation, E.B.; writing—original draft preparation, E.B.; writing—review and editing, F.C. and P.F.; visualization, E.B.; supervision, F.C.; project administration, F.C.. All authors have read and agreed to the published version of the manuscript."

Funding: This research received no external funding.

Data Availability Statement: Data are available on request.

Conflicts of Interest: The authors declare no conflict of interest.

References

1. Lo Giudice, R.; Galletti, C.; Tribst, J.P.M.; Melenchón, L.P.; Matarese, M.; Miniello, A.; Cucinotta, F.; Salmeri, F. In Vivo Analysis of Intraoral Scanner Precision Using Open-Source 3D Software. Prosthesis 2022, 4, 554–563, doi:10.3390/prosthesis4040045.
2. Cucinotta, F.; Raffaele, M.; Salmeri, F. A Topology Optimization of a Motorsport Safety Device. In; 2020; pp. 400–409.
3. Raj, T.; Hashim, F.H.; Huddin, A.B.; Ibrahim, M.F.; Hussain, A. A Survey on LiDAR Scanning Mechanisms. Electron. 2020, 9, doi:10.3390/electronics9050741.
4. Altadonna, A.; Cucinotta, F.; Raffaele, M.; Salmeri, F.; Sfravara, F. Environmental Impact Assessment of Different Manufacturing Technologies Oriented to Architectonic Recovery and Conservation of Cultural Heritage. Sustainability 2023, 15, 13487, doi:10.3390/su151813487.
5. Asheghi Bonabi, I.; Hemmati*, S. Bone Surface Model Development Based on Point Clouds Extracted From CT Scan Images. ADMT J. 2017, 10, 61–70.
6. Pan, Y.; Dong, Y.; Wang, D.; Chen, A.; Ye, Z. Three-Dimensional Reconstruction of Structural Surface Model of Heritage Bridges Using UAV-Based Photogrammetric Point Clouds. Remote Sens. 2019, 11, doi:10.3390/rs11101204.
7. Ahmed, S.; Chew, C. Density-Based Clustering for 3D Object Detection in Point Clouds. In Proceedings of the 2020 IEEE/CVF Conference on Computer Vision and Pattern Recognition (CVPR); 2020; pp. 10605–10614.
8. Xia, S.; Chen, D.; Wang, R.; Li, J.; Zhang, X. Geometric Primitives in LiDAR Point Clouds: A Review. IEEE J. Sel. Top. Appl. Earth Obs. Remote Sens. 2020, 13, 685–707, doi:10.1109/JSTARS.2020.2969119.
9. Guerrero, P.; Kleiman, Y.; Ovsjanikov, M.; Mitra, N.J. PCPNet Learning Local Shape Properties from Raw Point Clouds. Comput. Graph. Forum 2018, 37, 75–85, doi:10.1111/cgf.13343.
10. Hackel, T.; Wegner, J.D.; Schindler, K. Fast Semantic Segmentation of 3D Point Clouds With Strongly Varying Density. ISPRS Ann. Photogramm. Remote Sens. Spat. Inf. Sci. 2016, III–3, 177–184, doi:10.5194/isprsannals-iii-3-177-2016.
11. Shannon, C.E. A Mathematical Theory of Communication. Bell Syst. Tech. J. 1948, 27, 379–423, doi:10.1002/j.1538-7305.1948.tb01338.x.
12. Adolfsson, D.; Castellano-Quero, M.; Magnusson, M.; Lilienthal, A.J.; Andreasson, H. CorAl: Introspection for Robust Radar and Lidar Perception in Diverse Environments Using Differential Entropy. Rob. Auton. Syst. 2022, 155, 104136, doi:10.1016/j.robot.2022.104136.
13. Chen, D.-W.; Miao, R.; Yang, W.-Q.; Liang, Y.; Chen, H.-H.; Huang, L.; Deng, C.-J.; Han, N. A Feature Extraction Method Based on Differential Entropy and Linear Discriminant Analysis for Emotion Recognition. Sensors 2019, 19, 1631, doi:10.3390/s19071631.
14. Cover, T.M.; Thomas, J.A. Elements of Information Theory; John Wiley & Sons, Inc., 1991; ISBN 0471062596.

Disclaimer/